SELENIUM(IV) ELECTROCHEMISTRY ON SILVER: A COMBINED ELECTROCHEMICAL QUARTZ-CRYSTAL MICROBALANCE AND CYCLIC VOLTAMMETRIC INVESTIGATION

Giovanni PEZZATINI[1], Francesca LOGLIO[2], Massimo INNOCENTI[3] and Maria Luisa FORESTI[4,*]

Dipartimento di Chimica, Universitaà di Firenze, Via della Lastruccia 5, 5019 Sesto Fiorentino, Italy; e-mail: [1] giop@unifi.it, [2] logliof@unifi.it, [3] minnocenti@unifi.it, [4] foresti@unifi.it

Received May 15, 2003
Accepted August 13, 2003

Dedicated to Professor Sergio Roffia on the occasion of his retirement and in recognition of his contribution to electrochemistry.

The electrochemical behavior of Se(IV) on silver was investigated by cyclic voltammetry and electrochemical quartz-crystal microbalance (EQCM) measurements. As already reported in the literature, Se(IV) electrochemistry is always complex, and on silver even more, due to the formation of a compound. Our results confirm that the reduction process of Se(IV) occurs through two reaction paths, Se(IV) → Se(0) and Se(IV) → Se(–II); the product Se(–II) then reacts with Se(IV) through a comproportionation reaction. The latter step leads to red Se that, according to the literature, is the only electroactive form of Se(0). The presence of the electroactive red Se is evident both in the negative range of potentials, through the reduction Se(0) → Se(–II), and in the less negative range of potentials, through the oxidation Se(0) → Se(IV). Moreover, our measurements pointed to the formation of a deposit that never redissolves. This deposit seems to be the electroinactive gray Se. The electrochemical behavior of Se(IV) was investigated in the whole potential range accessible on silver. Our results confirm the occurrence of competitive processes whose predominance depends on the scan rate, as well as on the potential limits of voltammetry. A detailed table with the processes occurring in different potential ranges was drawn up.

Keywords: Selenium; EQCM; Silver; Electrodeposition; Cyclic voltammetry; Selenides; Electroreduction.

The electrochemical behavior of selenium on silver has been investigated in ammonia buffer solutions at pH 9.2. The investigation was carried out in the framework of electrodeposition of cadmium and zinc selenides on silver by electrochemical atomic layer epitaxy (ECALE) method[1,2]. The peculiarity of the method consists in using the underpotential deposition (UPD) phenomenon to deposit monolayers of the elements that form the compound [3,4].

The method is particularly suitable for the deposition of group II–VI compound semiconductors. From an experimental point of view, the conditions for the deposition must be thoroughly determined and controlled. The deposition of the metallic elements is performed through the reductive UPD from solutions containing the metal ions. Analogously, the deposition of sulfur layers is obtained by oxidative UPD from solution of sulfide ions. Unfortunately, the instability of selenide and telluride solutions does not allow oxidative depositions. Therefore, Se and Te UPD layers are obtained in a two-step procedure consisting of depositing an excess of Se or Te from Se(IV) or Te(IV) solutions, and of applying subsequently a potential sufficiently negative to reduce bulk Se or Te, but not UPD Se or Te. The reduction must be performed in the absence of Se(IV) or Te(IV) to avoid the comproportionation reactions with Se(–II) or Te(–II) leading to a massive formation of Se(0) or Te(0)[5–8]. Thus, after depositing Se(0) or Te(0), the Se(IV) or Te(IV) solutions must be replaced by a solution of the supporting electrolyte. The knowledge of the electrochemical behavior of Se(IV) and Te(IV) is therefore necessary to optimize the experimental conditions to obtain Se and Te UPD layers.

A wide overview of Se(IV) electrochemistry is given by Rajeshwar *et al.*[5] The Se(IV) electrochemical behavior is particularly complicated due to the concurrence of several factors. First of all, there are two possible reaction paths:

$$H_2SeO_3 + 4\ H^+ + 4\ e \Rightarrow Se + 3\ H_2O \qquad (1)$$

$$H_2SeO_3 + 6\ H^+ + 6\ e \Rightarrow H_2Se + 3\ H_2O\ . \qquad (2)$$

Literature data report the formation of at least two types of Se(0) associated with the reduction of Se(IV)[7,9]. In particular, gray selenium is attributed to the direct reduction (Eq. (*1*)), whereas red selenium is attributed to comproportionation reaction (*3*) (in an acidic medium)

$$H_2SeO_3 + 2\ H_2Se \rightarrow 3\ Se + 3\ H_2O \qquad (3)$$

or (*4*) (in an alkaline medium)

$$SeO_3^{2-} + 2\ Se^{2-} + 3\ H_2O \rightarrow 3\ Se + 6\ OH^- \qquad (4)$$

Elsewhere, it has been reported that gray Se deposited according to Eq. (*1*) is electroinactive[8]. A limited electroactivity of the reduction products of Se(IV) on graphite has already been reported[10–13]. Another complication is due to the tendency for passivation of the electrode surfaces[9–15].

As proposed by Kazacos and Miller[14], in acidic medium, the reduction of Se(IV) on various electrode materials (Hg, Cu, Ag, Au, Pt and graphite) proceeds according to Eq. (*2*) followed by comproportionation reaction (*3*). The rate of the chemical reaction depends on H_2SeO_3 concentration. At high concentrations, reaction (*3*) is so fast that the whole process appears to proceed through reaction (*1*), *e.g.* through a four-electron process. In addition, electrodes consisting of group II elements react with Se(IV) according to Eq. (*5*):

$$n\ M + H_2SeO_3 + 4\ H^+ + 4\ e \Rightarrow M_nSe + 3\ H_2O\ , \qquad (5)$$

where M = Hg, Ag, Cu; n = 1 for Hg and n = 2 for Ag or Cu.

Even more detailed is the mechanism proposed by Rajeshwar *et al.*[5] for the Se(IV) reduction on gold. From electrochemical quartz-crystal microbalance (EQCM) measurements combined with cyclic voltammetry, these authors have established that reactions (*1*) and (*2*) take place contemporarily at less negative potentials. The dominant reduction process taking place at more negative potentials is then attributed to the reduction of Se(0) produced by reaction (*3*). Rajeshwar's paper also takes into account the geometry of the electrochemical cell. In fact, as the electroreducing species is the chemically formed red selenium, the way in which its sedimentation occurs on the electrode is important. Thus, measurements carried out with a "face-down" electrode configuration revealed a markedly diminished reduction process, due to the hindered sedimentation compared to the "face-up" configuration[5].

More recently, an EQCM investigation of Se(IV) electrochemistry was performed in the framework of the thin-film electrodeposition of $Cu_{2-x}Se$ on gold[16].

EXPERIMENTAL

Instrumentation

Analytical reagent-grade $Na_2SeO_3 \cdot 5H_2O$ (Fluka) was used without further purification. Analytical reagent-grade $HClO_4$ and NH_3 (both Merck) served for preparation of the pH 9.2 ammonia buffer employed as supporting electrolyte. The water used was obtained from mineral water by single distillation and then by distillation of the obtained water from alkaline permanganate while constantly discarding the heads. The solutions were freshly prepared just

before the beginning of each series of measurements. Before use, the solutions were thermostatted and deoxygenated by purging with nitrogen gas.

A CH Instruments Model 604a Electrochemical Analyzer was used either in conjunction with the EQCM or to record cyclic voltammograms and differential capacity curves. Cyclic voltammetry was run either using massive silver electrodes or EQCM electrodes coated with silver. Massive silver electrodes, both polycrystalline and single-crystal, were grown by the Bridgman technique and cut as to form discs *ca* 1 cm in diameter[17,18]. Before their use, the working electrodes were treated with a chemical etching based on CrO_3 (ref.[19]). The working electrodes were placed in a flow-cell connected to an automated and computerized system for the solution exchange described elsewhere[20].

EQCM measurements were carried out using the basic instrument supplied by Seiko EG&EG (QCA917). The working electrode was a 9-MHz AT-cut quartz crystal with silver electrode furnished by Ditta Nuova Mistral (Latina, Italy). The diameter of the quartz crystal was 14.0 mm and that of the silver electrode 7.4 mm. The area of the working electrode in contact with solution was limited to 0.43 cm^2 by an O-ring. The silver electrode on the crystals consisted of a 300-nm Ag sputter deposited on an adhesion layer of 50-nm Ti. A suitable flow-cell entirely made of Teflon was designed and realized in the workshop of the Department.

The counter-electrode was a gold foil, and the reference electrode an Ag|AgCl|3 M KCl (E = 0.205 V *vs* NHE) placed on the outlet tubing of the cell.

Characterization and Suggested Pre-Treatment of EQCM Electrodes

The commercial EQCM electrodes were treated by alternate immersions in 25% NH_3, 96% H_2SO_4 and again 25% NH_3, with intermediate washing steps. Differential capacitance curves recorded in 5×10^{-2} M $NaClO_4$, before and after the above treatment, showed the evolution from a flat curve to that showing a minimum at about –0.95 V. This minimum is consistent with the potential of zero charge of polycrystalline silver substrates (Fig. 1). The morphology of the EQCM electrodes was monitored by AFM measurements carried out with

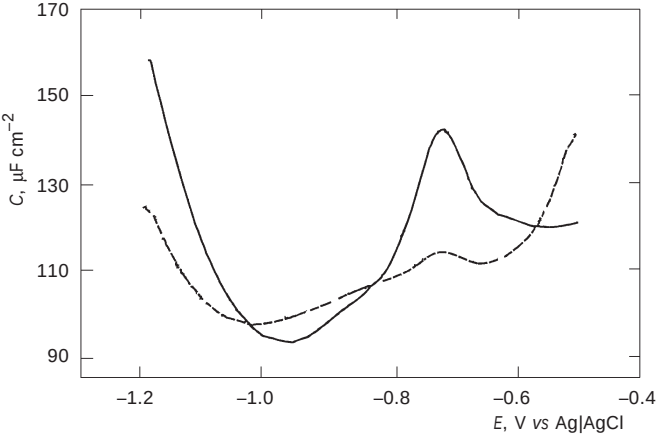

FIG. 1
Differential capacitance curves of silver-covered EQCM quartz crystals recorded before (dashed curve) and after (solid curve) the chemical treatment

a Pico SPM (Molecular Imaging) operating in contact mode, with a commercial Si_3N_4 cantilever (Nanosensors, Wetzlar–Blankenfeld). Figure 2 shows 25 × 25 μm^2 three-dimensional AFM images before and after the treatment: the effective smoothing of the surface is indicated by the strong lowering of the root mean square roughness from 191 to 117 nm. After the treatment, the roughness factor, R_f = physical area/geometric area, is approximately 1.5.

RESULTS AND DISCUSSION

As already stated, this study is devoted to the elucidation of the Se(IV) electrochemical behavior to optimize the experimental conditions of growing cadmium and zinc selenides on silver by the ECALE methodology. In our laboratory, these compounds were grown on Ag(111). The use of single crystals as substrates increases the probability of the epitaxial growth and, hence, the attainment of well-structured compounds[1,2]. On the other hand, EQCM measurements were performed on commercial silver-covered quartz crystals. The silver deposit is polycrystalline and has a very high roughness. For this reason, EQCM measurements were integrated by a comparative electrochemical investigation on massive mono- and polycrystalline silver, as well as on EQCM electrodes.

Figure 3a shows the progressive evolution of cyclic voltammograms as obtained by a continuous scan from –0.1 to –1.1 V on Ag(111). To better stress the evolution, Fig. 3b shows an enlargement of the curve obtained on a fresh substrate after having kept the electrode at the initial potential E = –0.1 for 10 min, and Fig. 3c shows the curve obtained after eight successive scans. Peaks C1 and C2 observed in the first scan tend to progressively diminish and, eventually, completely disappear. At the same time, a third peak, C3, appears. The charge involved in peak C3 reaches a limiting value

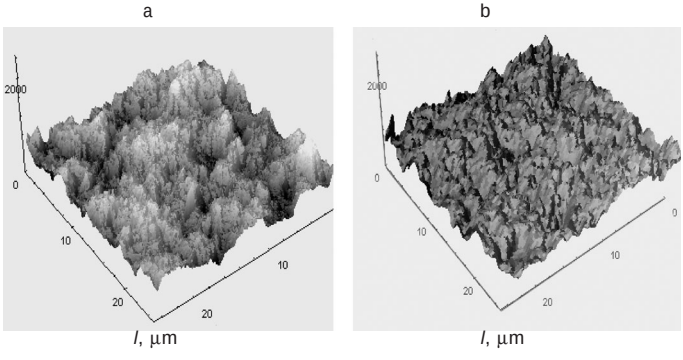

FIG. 2
25 × 25 μm^2 three-dimensional AFM images of silver-covered EQCM quartz crystals before (a) and after (b) the chemical treatment

that depends on SeO_3^{2-} concentration. The attainment of a constant charge value is not detected at first sight in Fig. 3a. However, it must be noted that cathodic currents are increasing both in the forward and the backward scans. Thus, the peak area, and therefore the charge, remain constant. The first backward scan shows an anodic peak at –0.57 V (Fig. 3b). The successive backward scans show one peak at –0.77 V (A1), and a second broad and hardly visible peak (A2) between –0.4 and –0.2 (Fig. 3c).

From a general point of view, these peaks are neither associated with the crystallographic orientation of silver, nor with its quality. The only differences between mono- and polycrystalline silver consist in small potential

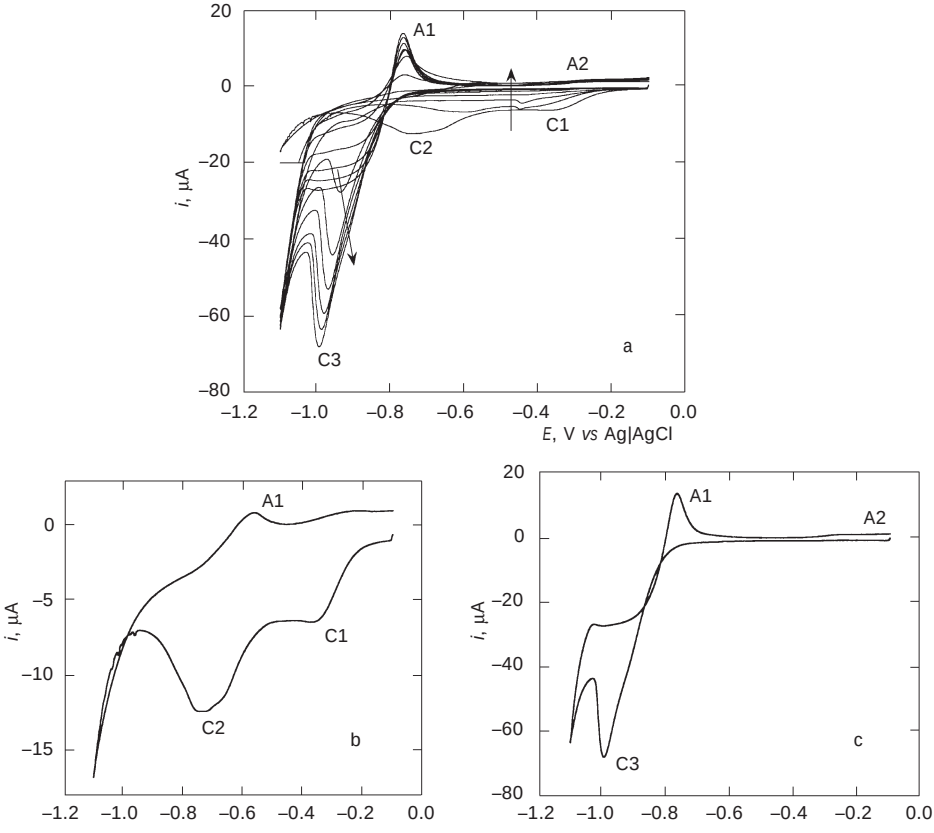

FIG. 3

Consecutive cyclic voltammograms of 8×10^{-4} M Se(IV) solutions in pH 9.3 ammonia buffer, recorded from –0.1 to –1.1 V *vs* Ag|AgCl on Ag(111) (a); first scan of this series recorded on a fresh electrode after having kept the electrode at $E = -0.1$ V for 10 min (b); ninth scan (c). The scan rate is 50 mV s^{-1}. The arrows in a indicate the evolution of the curves

shifts of the peaks observed in the first scan. This is probably due to the fact that the corresponding processes involve no more than one monolayer and, therefore, they experience the fine structure of the substrate. Figure 4 shows the comparison between the first scan obtained either on a fresh single crystal or on a fresh massive polycrystal. The peak at –0.57 V is not observed on polycrystal. However, an enlargement of the curve shows a small peak at –0.4 V. Both curves were recorded after having kept the electrode at the initial potential, E = –0.1, for 10 min. A time of 8–10 min is necessary for C1 to reach its limiting value in 8×10^{-4} M SeO_3^{2-}.

Figure 5 shows that C1 increases, while keeping the electrode at the initial potential for increasing times before the scan. To avoid involvement of peak C2, the scan was limited to –0.6 V. Analogous curves were recorded just after keeping the electrode in SeO_3^{2-} at the open circuit potential. It is therefore reasonable to attribute peak C1 to the reduction of the product of a chemical reaction. Incidentally, the open circuit potential, as measured just after introducing the SeO_3^{2-} solution, changes from a slightly negative value up to +0.056 V, indicating a spontaneous reduction process. Apart from a small change in the peak potentials, the same behavior was observed on all silver substrates examined.

As already stated, Kazacos and Miller[14] report on the Ag_2Se formation according to Eq. (*5*) when performing the cyclic voltammetry of Se(IV) on silver in 1 M H_2SO_4. Their hypothesis is based on the presence of a cathodic peak at *ca* +0.2 V *vs* SCE. Then, they observed a large cathodic peak at –0.6 V

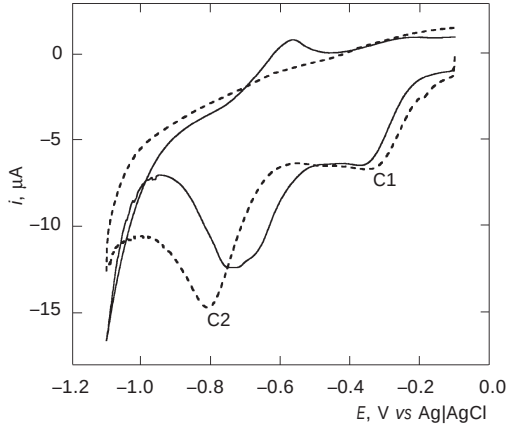

FIG. 4
Cyclic voltammograms of Se(IV) recorded from –0.1 to –1.1 V on Ag(111) (solid line) and on a massive polycrystalline silver (dashed line). Each curve was recorded after having kept the electrode at E = –0.1 V for 10 min

vs SCE, attributed to the reduction of Ag_2Se with H_2Se evolution. Considering the different medium used, the peak at +0.2 V could correspond to our peak C1. On the contrary, in our opinion, the hypothesis of Ag^+ reduction at potentials as negative as –0.6 V is to be disregarded, regardless the medium used. In this respect, EQCM measurements become decisive for the assignment of peaks C1 and C2. Figure 6 shows the frequency plot com-

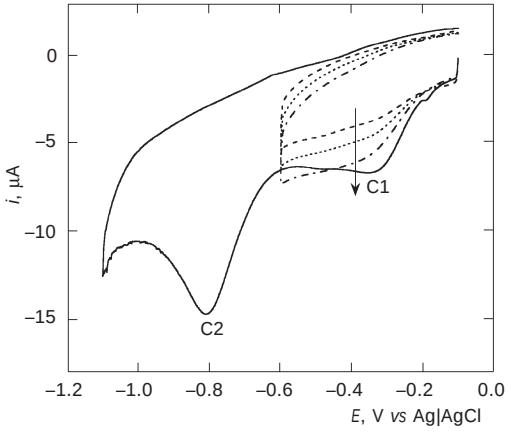

FIG. 5
Cyclic voltammograms of Se(IV) on polycrystalline silver electrode after having kept the electrode at E = –0.1 V for times ranging from 1 to 10 min, as given by the arrow

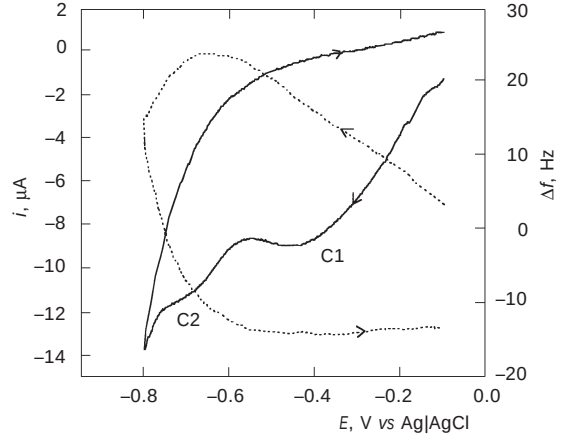

FIG. 6
Cyclic voltammograms obtained on a fresh silver-covered EQCM electrode from the same Se(IV) solution as in preceding Figures (solid line) and the corresponding frequency change (dashed line)

bined with the cyclic voltammogram. Keeping in mind that a frequency increase corresponds to mass loss, it is evident that the reduction process associated with peak C1 leads to some redissolution, rather than deposition processes. Therefore, this seems to exclude the fact that peak C1 corresponds to the formation of Ag_2Se. On the contrary, we might assume that Ag_2Se is formed before the potential scan, and that peak C1 corresponds to the reduction of Ag^+, with a release of Se(–II). The scanty frequency variation measured (20 Hz) does not allow for the precise calculation of the mass change involved. However, we have calculated that the release of Se(–II) corresponds to a mass loss equal to approximately 78 ng cm^{-2}. This value was obtained by considering the 2:1 stoichiometric ratio between silver and selenium. We approximated the atomic density of EQCM silver electrode to be that of the (100) crystallographic orientation, which is 1.2×10^{15} atoms cm^{-2}. The frequency variation (14 Hz) associated to this mass variation is given by the Sauerbrey equation:

$$\Delta f = -C_f \, \Delta m / A \, . \qquad (6)$$

Here, A is the electrode area, and C_f is a coefficient that depends on the quartz properties and on the fundamental resonance frequency. In our case, $C_f = 0.183$ Hz cm^2 ng^{-1}. Considering the high roughness factor (≈1.5), the experimental frequency change agrees with the calculated change. No such behavior was observed in experiments performed on the supporting electrolyte alone. Then, we can attribute all the described processes to the presence of selenium. Of course, the frequency change might also be produced by adsorption/desorption processes. Therefore, the frequency should also be monitored immediately after introducing Se(IV). Unfortunately, the perturbation caused by the solution flow prevents this check.

Figure 7a shows another experiment where three successive cyclic voltammograms were recorded after having kept the electrode at $E = -0.1$ V for 10 min before each scan. A progressive inhibition of peaks C1 and C2 is evident. The associated nanobalance response is reported in Fig. 7b. Reading together the two figures, it may be hypothesized that the Ag_2Se chemically formed on a fresh electrode is dissolved in the first scan between –0.1 and *ca* –0.65 V. At more negative potentials, the mass increase indicates some deposition processes. This mass increase is associated with peak C2 that presumably corresponds to Se(0) deposition. After inverting the scan, the mass continues to increase up to –0.6 V, after this value remaining constant. The absence of anodic peaks in the first cyclic voltammogram indicates that no redissolution occurs of what was formed during the cathodic

scan. This is the first indication of the lack of electroactivity of the electrochemically formed Se(0). Peak C1 is markedly lowered in the second scan and practically disappears in the third one. Correspondingly, no mass variation is observed. This would indicate some inhibition of the surface. No similar inhibition was observed in the curves depicted in Fig. 5, where the potential scan was limited to –0.6 V. Hence, we might assume a progressive blocking of the surface due to Se(0) deposition. The deposition process involving mass increase is clearly shown by the nanobalance response at negative potentials of *ca* –0.6 V. However, this result contrasts with the

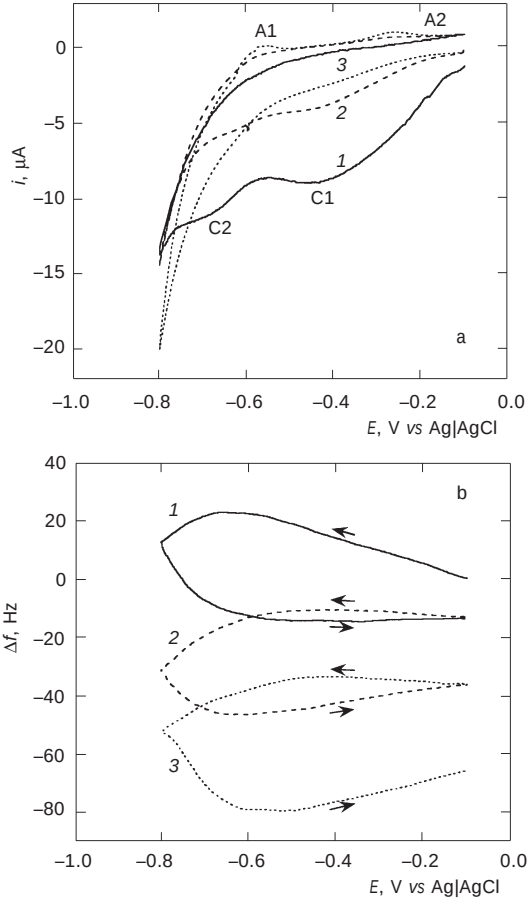

FIG. 7

Consecutive cyclic voltammograms of Se(IV) on silver-covered EQCM electrode (a) and corresponding frequency curves (b). Each curve was recorded after having kept the electrode at E = –0.1 V for 10 min before the scan

lowering of peak C2, that is of the electrochemically formed Se(0). Therefore, the mass increase seems to be determined by the concomitant deposition of the chemically formed Se(0) (red Se), specifically the product of the comproportionation reactions (*3*) or (*4*). This implies that some amount of Se(–II) must have been formed, which is not justified by the simple dissolution of Ag_2Se. As a consequence, the mechanism through the two reactions (*1*) and (*2*) seems to be proven. Further confirmation is given by the presence of the small anodic peak at about –0.6 V (A1), which indicates the reoxidation Se(–II) ⇒ Se(0). In other words, the mass increase is due to Se(0) deposition. However, the source of Se(0) has three different origins: (i) electroreduction of Se(IV); (ii) comproportionation reaction between Se(IV) and Se(–II); (iii) reoxidation of Se(–II). The potential regions where these reactions take place, partially overlap.

The third scan in Fig. 7a also shows an anodic peak at E = –0.3 V (A2) that involves a mass decrease.

To assign this peak, a more detailed analyses of massive polycrystalline silver substrate, as well as of Ag(111), were carried out. Figure 8a shows the cyclic voltammograms obtained after having kept the massive polycrystal at potentials in the range –0.6 to –0.8 V for 2 min, and subsequently having scanned the potential from –0.8 to –0.1 V. The anodic scans, obtained after having kept the electrode at less negative potentials (–0.6, –0.65 and –0.7 V) show a series of peaks between –0.7 and –0.4 V. After having kept the electrode at more negative potentials (–0.75 and –0.8 V), these peaks are progressively reduced in favor of a more defined anodic peak at E = –0.75 V (A1) and another anodic peak at –0.3 V (A2). Peaks A1 and A2 correspond to those of Fig. 7a, the small differences in the potential values being due to the normal mass effect and to the different scan rate. It is interesting to note that peak A2 is definitely associated with A1, specifically that it increases with an increase of A1. Thus, at first sight, A2 seems to indicate the reoxidation process of Se(0) formed at A1. Considering the standard potential for the Se(IV)/Se(0) system equal to +0.74 V *vs* SHE at pH 0 and to –0.366 V *vs* SHE at pH 14 (ref.[21]), our value E = –0.3 V *vs* Ag|AgCl is consistent with pH 9.2 for our measurements. However, the charge involved in peak A2 is constantly lower than that involved in A1. Yet, the oxidation Se(0) ⇒ Se(IV) involves four electrons, whereas the oxidation Se(–II) ⇒ Se(0) just two electrons. Neither cyclic voltammetry nor EQCM measurements are able to explain this discrepancy. A tentative explanation might be a lack of electroactivity of Se(0) formed by Se(–II) reoxidation, as in the case of Se(0) formed by Se(IV) reduction. Thus, the species that undergoes oxidation might be the chemically formed Se(0). The latter is unavoidably

present, due to the concomitant comproportionation reaction. This conclusion is supported by the fact that, as shown in Fig 7b, continuous cycling between –0.1 and –0.8 V leads to a resulting increase in mass, thus indicating that most of the deposited Se(0) is not reoxidized. The small size of peak A2 confirms this indication. Moreover, peak A2 does not appear immediately, which is consistent with the need for a significant formation of Se(–II) to trigger the chemical Se(0) formation. Thus, the above mentioned association with peak A1 does not imply that what is formed in A1 is

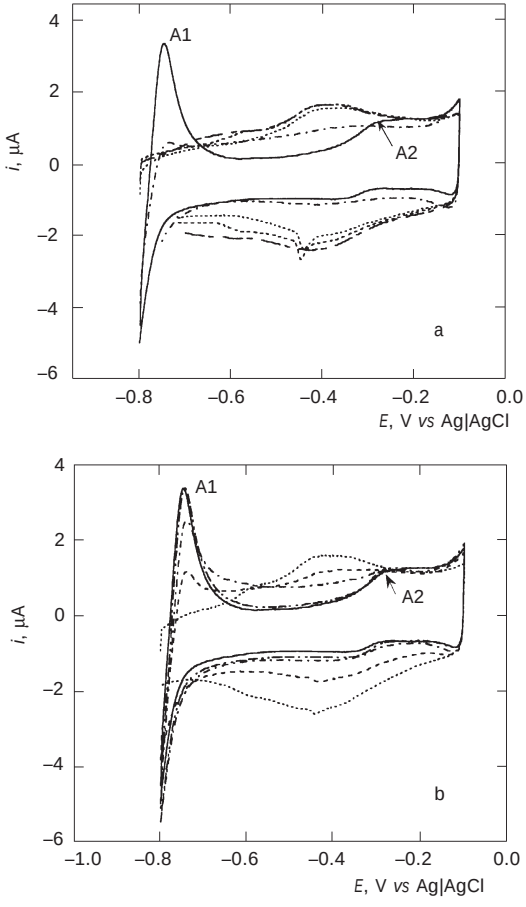

FIG. 8

Cyclic voltammograms of Se(IV) recorded from –0.8 to –0.1 V on massive polycrystalline silver electrode. The curves were recorded after having kept the electrode for 2 min at –0.60 (- — -), –0.65 (- - -), –0.70 (····), –0.75 (–··–), –0.80 (—) V (a); after having kept the electrode at E = –0.8 V for 0.5 (····), 1 (- - -), 1.5 (–·–), 2 (–··–), 2.5 (—) min (b)

reoxidized in A2, but rather indicates that A2 needs Se(–II), whose presence is revealed by A1. Incidentally, the fact that A1 appears only after applying a sufficiently negative potential suggests that reaction (*2*) occurs at more negative potentials than reaction (*1*).

The presence of a deposit on the surface is also indicated by the decreasing current, which points to a change in the capacitive contribution. It is also interesting to note the small cathodic peak at *ca* –0.43 V in Fig. 8a. This peak is observed only on curves where the extent of Se(0) deposition is limited. This fact, and the almost well defined shape of the peak, might indicate a phase transition.

An analogous experiment, where the electrode was kept at –0.8 V while increasing time delay before the scan, shows that peak currents of A1 and A2 reach a limiting value. This value is presumably connected to the maximum concentration of Se(–II) which is possible to obtain at E = –0.8 V through reaction (*2*) for the Se(IV) concentration used (Fig. 8b).

Analogous evolution towards the formation of peaks A1 and A2 is observed on Ag(111). The only difference is that the single crystal has only one initial peak at –0.57 V, whereas the polycrystal has a series of peaks between –0.7 and –0.4 V. This observation implies that the presence of such peaks is associated with the fine structure of the substrate.

At potentials more negative than –0.8 V, red Se(0) is reduced to Se(–II) (peak C3 in Fig. 3). In turn, Se(–II) reacts with Se(IV), giving more red Se(0). Then, we have two competitive effects: (i) mass increase, due to formation of Se(0) (gray from Se(IV), and red from the comproportionation reaction); (ii) mass decrease due to the reduction of red Se(0). The resulting effect depends on the applied potential. If the potential is varied, as in the case of cyclic voltammetry, it depends on the scan rate, as well as on the chosen potential limits.

Figure 9a shows the Δf *vs* E plot corresponding to the voltammogram of Fig. 9b recorded at 2 mV s^{-1}. The various processes occurring in the potential range –0.1 to –1.4 V at this extremely low scan rate are summarized in Table I. It must be noted that the resulting mass balance on a fresh electrode is a mass increase, regardless the scan rate used.

Figure 10 shows the Δf *vs* E curves of four consecutive cyclic voltammograms, recorded at a scan rate of 50 mV s^{-1}. The first curve was recorded on a fresh electrode after having applied E = –0.1 V for 10 min. The following curves were recorded in succession. For this reason, the mass decrease associated with Ag_2Se dissolution is only observed in the first scan. Note that a Δf decrease corresponds to a mass increase, and that the resulting balance of the four scans is a mass increase. However, it must be noted that the

shape of the curves gradually changes. At lower scan rates, these changes are even more marked, and the resulting mass balance in similar successions of curves may also be a mass decrease. This again indicates the occurrence of competitive processes whose predominance depends of the scan rate, as well as on the potential limits. Incidentally, after the experiments the electrodes looked gray, with a deposited film whose thickness depended

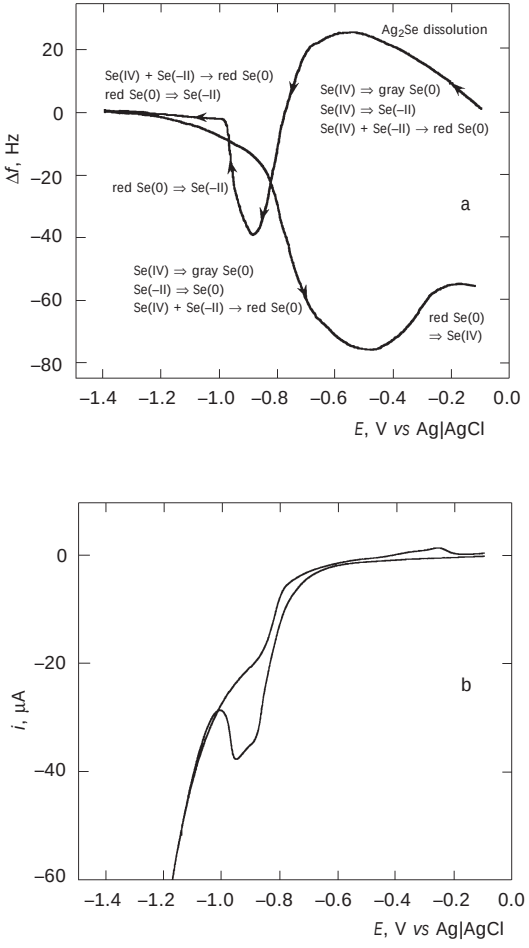

FIG. 9

Frequency change during a single potential scan from –0.1 to –1.4 V, recorded on the silver EQCM electrode from the same Se(IV) solution as in preceding Figures (a) and the corresponding cyclic voltammogram with the same electrode (b). The curve was recorded after having kept the electrode at E = –0.1 V for 10 min. The scan rate was 2 mV s^{-1}

TABLE I
The processes occurring in the potential range –0.1 to –1.4 V

Potential range	Process	Assignment
Forward scan		
–0.1 to –0.6 V	mass decrease	Ag_2Se reduction with Se(–II) release
–0.6 to –0.9 V	large mass increase	Se(IV) ⇒ gray Se(0) Se(IV) ⇒ Se(–II) Se(IV) + Se(–II) → red Se(0)
–0.9 to –1.0 V	large mass decrease	the reduction of red Se(0) prevails over its formation
–1.0 to –1.4	no mass change	the rate of formation of red Se(0) is approximately equal to the rate at which it is consumed
Backward scan		
–1.4 to –0.85 V	slight mass increase	the formation of red Se(0) prevails over its reduction
–0.85 to –0.5	large mass increase	Se(IV) ⇒ gray Se(0) Se(–II) ⇒ gray Se(0) Se(IV) + Se(–II) → red Se(0) (the reduction of red Se(0) is over
–0.5 to –0.1 V	mass decrease	red Se(0) ⇒ Se(IV)

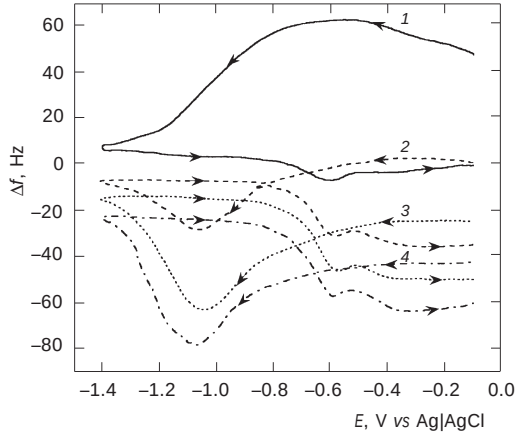

FIG. 10
Frequency curves of four consecutive potential scans from –0.1 to –1.4 V at the scan rate equal to 50 mV s^{-1}

on the time interval the electrodes were used. In principle, due to the similar gray color, the co-presence of some Ag_2Se cannot be excluded. However, relatively thick gray deposits could also be observed after having kept the electrode at potentials where Ag^+ is surely reduced.

CONCLUSIONS

The electrochemical behavior of Se(IV) on silver was investigated by cyclic voltammetry and EQCM measurements. As already reported in the literature for other substrates, Se(IV) electrochemistry is complex.

As summarized in Table I, our results confirm that the reduction of Se(IV) occurs through the two reactions (*1*) and (*2*). The results also confirm that the Se(–II) formed by reaction (*2*) reacts with Se(IV) through comproportionation. The latter reaction produces red Se that, according to the literature, is the only electroactive form of Se(0).

On silver electrodes, the situation is complicated by the formation of a compound. Our results are consistent with the hypothesis[14] that the compound formed is Ag_2Se. However, EQCM measurements in correspondence to the voltammetric peak associated with the presence of Ag_2Se show a decrease of mass. Therefore, some redissolution, rather than deposition, is indicated. This circumstance, together with the likely formation of the compound also at the open circuit potential, may evoke that the compound is formed chemically. All measurements carried out in the potential range –0.1 to –1.4 V indicate the formation of a deposit that never redissolves. This deposit seems to be the electroinactive gray Se. The presence of the electroactive red Se is evident both in the more negative potential range, through the reduction Se(0) ⇒ Se(–II), and in the less negative potential range, through the oxidation Se(–II) ⇒ Se(IV).

The comparison with measurements performed in the absence of selenite allows the assignment of the described mass changes to processes involving selenium.

The authors are grateful to Mr A. Pozzi and Mr F. Gualchieri for their technical assistance, and to Mr F. Capolupo for the preparation of the silver single-crystal electrodes. The financial support of the Italian CNR, of the Murst and of the Consorzio Interuniversitario per la Scienza e Tecnologia (INSTM) is gratefully acknowledged.

REFERENCES

1. Pezzatini G., Caporali S., Innocenti M., Foresti M. L.: *J. Electroanal. Chem.* **1999**, *475*, 164.

2. Loglio F., Innocenti M., Pezzatini G., Forni F., Foresti M. L.: *Experimental Conditions for CdSe Layer-by-Layer Growth*, Proceeding Vol. 8. Electrochemical Society Inc., Toronto 2000.
3. Gregory B. W., Stickney J. L.: *J. Electroanal. Chem.* **1991**, *300*, 543.
4. Stickney J. L. in: *Electroanalytical Chemistry* (A. J. Bard and I. Rubinstein, Eds), Vol. 21. Marcel Dekker, New York 1999.
5. Wei C., Myung N., Rajeshwar K.: *J. Electroanal. Chem.* **1994**, *375*, 109.
6. Tomkiewicz M., Ling I., Parsons W. S.: *J. Electrochem. Soc.* **1982**, *129*, 2016.
7. Espinosa A. M., Toscon M. L., Vazquez M. D., Batanero P. S.: *Electrochim. Acta* **1992**, *37*, 1165.
8. Liu D., Zhang Y., Zhou S.: *J. Xiamen Univ.* **1989**, *28*, 495; *Chem. Abstr.* **1990**, *113*, 67284.
9. Jarzabek G., Kublik Z.: *J. Electroanal. Chem.* **1980**, *114*, 165.
10. Krapivkina T. A., Roizenblot E. M., Kalambet G., Nosatcheva V. V.: *Zh. Anal. Khim.* **1977**, *32*, 93.
11. Lunev M. I., Kamenov A. I., Agasyam P. K.: *Zh. Anal. Khim.* **1976**, *31*, 1476.
12. Kamenov A. I., Lunev M. I., Agasyam P. K.: *Zh. Anal. Khim.* **1977**, *32*, 550.
13. Portnyagina E. O., Stromberg A. G., Kaplin A. A.: *Zh. Anal. Khim.* **1984**, *39*, 493.
14. Kazacos M. S., Miller B.: *J. Electrochem. Soc.* **1980**, *127*, 869.
15. Mishra K. K., Rajeshwar K.: *J. Electroanal. Chem.* **1989**, *273*, 169.
16. Kemell M., Saloniemi H., Ritala M., Leskelä M.: *Electrochim. Acta* **2000**, *45*, 3737.
17. Hamelin A. in: *Modern Aspects of Electrochemistry* (B. E. Conway, R. E. White and J. O'M. Bockris, Eds), Vol. 16, p. 1. Plenum Press, New York 1985.
18. Foresti M. L., Capolupo F., Innocenti M., Loglio F.: *Cryst. Growth Des.* **2002**, *2*, 73.
19. Hamelin A., Stoicoviciu L., Doubova L., Trasatti S.: *J. Electroanal. Chem.* **1988**, *244*, 133.
20. Innocenti M., Pezzatini G., Forni F., Foresti M. L.: *J. Electrochem. Soc.* **2001**, *148*, C357.
21. Latimer W. M.: *The Oxidation States of the Elements and Their Potentials in Aqueous Solutions*, 2nd ed. Prentice-Hall, New York 1952.